# PI3K/p110δ is a novel therapeutic target in multiple myeloma

Hiroshi Ikeda,[1,2] Teru Hideshima,[1] Mariateresa Fulciniti,[1] Giulia Perrone,[1] Naoya Miura,[1] Hiroshi Yasui,[1,2] Yutaka Okawa,[1] Tanyel Kiziltepe,[1] Loredana Santo,[1] Sonia Vallet,[1] Diana Cristea,[1] Elisabetta Calabrese,[1] Gullu Gorgun,[1] Noopur S. Raje,[1] Paul Richardson,[1] Nikhil C. Munshi,[1,3] Brian J. Lannutti,[4] Kamal D. Puri,[4] Neill A. Giese,[4] and Kenneth C. Anderson[1]

[1]Lebow Institute for Myeloma Therapeutics and Jerome Lipper Multiple Myeloma Center, Department of Medical Oncology, Dana-Farber Cancer Institute, Harvard Medical School, Boston, MA; [2]First Department of Internal Medicine, Sapporo Medical University S-1, Sapporo, Japan; [3]Boston VA Healthcare System, West Roxbury, MA; and [4]Calistoga Pharmaceuticals Inc, Seattle, WA

**In this study, we demonstrate expression and examined the biologic sequelae of PI3K/p110δ signaling in multiple myeloma (MM). Knockdown of p110δ by small interfering RNA caused significant inhibition of MM cell growth. Similarly, p110δ specific small molecule inhibitor CAL-101 triggered cytotoxicity against LB and INA-6 MM cell lines and patient MM cells, associated with inhibition of Akt phosphorylation. In contrast, CAL-101 did not inhibit survival of normal peripheral blood mononuclear cells. CAL-101 overcame MM cell growth conferred by interleukin-6, insulin-like growth factor-1, and bone marrow stromal cell coculture. Interestingly, inhibition of p110δ potently induced autophagy. The in vivo inhibition of p110δ with IC488743 was evaluated in 2 murine xenograft models of human MM: SCID mice bearing human MM cells subcutaneously and the SCID-hu model, in which human MM cells are injected within a human bone chip implanted subcutaneously in SCID mice. IC488743 significantly inhibited tumor growth and prolonged host survival in both models. Finally, combined CAL-101 with bortezomib induced synergistic cytotoxicity against MM cells. Our studies therefore show that PI3K/p110δ is a novel therapeutic target in MM and provide the basis for clinical evaluation of CAL-101 to improve patient outcome in MM. (*Blood*. 2010;116(9): 1460-1468)**

## Introduction

The bone marrow (BM) microenvironment plays a crucial role in pathogenesis of multiple myeloma (MM) by promoting cell proliferation, survival, migration, and drug resistance.[1-4] The PI3K/AKT pathway mediates growth and drug resistance in MM cells and also plays a significant role in autophagy.[5,6] PI3K is activated via upstream tyrosine kinase-associated receptors for growth factors, cytokines, antigens, and costimulatory molecules. It in turn activates AKT, which mediates cell proliferation, cell cycle, apoptosis, and autophagy.[7] Class IA PI3K consists of 5 isoforms of regulatory subunits (p85α, p50α, p55α, p85β, and p55γ), which interact with class IA isoforms. Class IA PI3K is composed of p110α, -β, and -δ isoforms.[8] Among the 8 distinct mammalian isoforms of PI3K, class I PI3Ks are responsible for Akt activation. Importantly, p110δ is expressed in many cancers, including colon and bladder carcinoma, glioblastoma, and acute myeloid leukemia blasts.[9,10]

In the current study, we demonstrate high expression of p110δ in patient MM cells. Previous studies have shown that CAL-101, a potent and selective p110δ inhibitor, has broad antitumor activity against cancer cells of hematologic origin.[11,12] Moreover, inhibition of p110δ induces cleavage of caspases and LC3, consistent with apoptotic and autophagic cell death, respectively. Here we show that p110δ blockade with CAL-101, a potent and selective p110δ inhibitor, inhibits MM cell growth even in the presence of interleukin-6 (IL-6), insulin-like growth factor-1 (IGF-1), or bone marrow stromal cells (BMSCs), associated with decreased phosphorylation of AKT and P70S6k. We also confirmed inhibition of human MM cell growth triggered by p110δ inhibition in our xenograft mouse models of human MM. These studies therefore show that small molecule inhibitors of p110δ trigger significant anti-MM cytotoxicity both in vitro and in vivo, providing the framework for their clinical evaluation to improve patient outcome in MM.

## Methods

### Materials

p110δ inhibitor CAL-101 and IC488743 were provided by Calistoga Pharmaceuticals. CAL-101 was dissolved in dimethyl sulphoxide at 10mM and stored at −20°C for in vitro study. IC488743 was dissolved in 1% carboxyl methylcellulose/0.5% Tween 80 and stored at 4°C for in vivo study. Recombinant human p110α, β, γ, and δ were reconstituted with sterile phosphate-buffered saline (PBS) containing 0.1% bovine serum albumin. Bortezomib was provided by Millennium Pharmaceuticals. 3-Methyladenine was purchased from Sigma-Aldrich.

### Cell culture

Dex-sensitive (MM.1S) and Dex-resistant (MM.1R) human MM cell lines were kindly provided by Dr Steven Rosen (Northwestern University, Chicago, IL). H929, RPMI8226, and U266 human MM cell lines were obtained from ATCC. Melphalan-resistant RPMI-LR5 and doxorubicin (Dox)-resistant RPMI-Dox40 cell lines were kindly provided by Dr William Dalton (Lee Moffitt Cancer Center, Tampa, FL). OPM1 plasma cell leukemia cells were provided by Dr Edward Thompson (University of Texas Medical Branch, Galveston). IL-6–dependent human MM cell line INA-6 was provided by Dr Renate Burger (University of Kiel, Kiel,

Submitted June 8, 2009; accepted November 30, 2009. Prepublished online as *Blood* First Edition paper, May 26, 2010; DOI 10.1182/blood-2009-06-222943.

The online version of this article contains a data supplement.

The publication costs of this article were defrayed in part by page charge payment. Therefore, and solely to indicate this fact, this article is hereby marked "advertisement" in accordance with 18 USC section 1734.

Germany). LB human MM cell line was established in our laboratory. No cytogenetic abnormalities were found; phenotypic analysis is shown in supplemental Figure 1 (available on the *Blood* Web site; see the Supplemental Materials link at the top of the online article). All MM cell lines were cultured in RPMI 1640 medium. BMSCs were cultured in Dulbecco modified Eagle medium (Sigma-Aldrich) containing 15% fetal bovine serum, 2mM L-glutamine (Invitrogen), 100 U/mL penicillin, and 100 μg/mL streptomycin (Invitrogen). Blood samples collected from healthy volunteers were processed by Ficoll-Paque gradient to obtain peripheral blood mononuclear cells (PBMCs). Patient MM and BM cells were obtained from BM samples after informed consent was obtained in accordance with the Declaration of Helsinki and approval by the Institutional Review Board of the Dana-Farber Cancer Institute. BM mononuclear cells were separated using Ficoll Paque density sedimentation, and plasma cells were purified (> 95% $CD138^+$) by positive selection with anti-CD138 magnetic activated cell separation microbeads (Miltenyi Biotec). Tumor cells were also purified from the BM of MM patients using the RosetteSep negative selection system (StemCell Technologies), as described previously.[13,14]

### Growth inhibition assay

The growth inhibitory effect of CAL-101 on growth of MM cell lines, PBMCs, and BMSCs was assessed by measuring 3-(4,5-dimethylthiazol-2-yl)-2,5-diphenyl tetra-sodium bromide (MTT; Chemicon International) dye absorbance, as previously described.[13]

### Effect of CAL-101 on paracrine MM cell growth in the BM

MM cells ($2 \times 10^4$ cells/well) were cultured for 48 hours in BMSC-coated 96-well plates (Corning Life Sciences) in the presence or absence of drug. DNA synthesis was measured by [$^3$H]-thymidine (PerkinElmer Life and Analytical Sciences) uptake, with added (0.5 μCi/well) during the last 8 hours of 48-hour cultures. All experiments were performed in quadruplicate.

### Transient knockdown of p110δ expression

INA-6 cells were transiently transfected with siRNA ON-TARGET plus SMART pool p110δ or nonspecific control duplex (Dharmacon RNA Technologies) using Cell Line Nucleofector Kit V (Amaxa Biosystems), as described previously.[15]

### Electron microscopy

Cells were collected and fixed with 2.0% paraformaldehyde/2.5% electron microscope grade glutaraldehyde in 0.1M sodium cacodylate buffer (pH 7.4) at 37°C. After fixation, samples were placed in 2% osmium tetroxide in 0.1M sodium cacodylate buffer (pH 7.4), dehydrated in a graded series of ethyl alcohol, and embedded in resin. Ultrathin sections were cut and placed on formvar-coated slot copper grids. Sections were then counterstained with uranyl acetate and lead citrate, and viewed with a TecnaiTM G2 Spirit Bio TWIN electron microscope. Digital images were acquired with an AMT 2k CCD camera (direct original magnifications, ×1400 and ×6800).

### Immunofluorescence

Viable MM cells ($2.5 \times 10^4$) were pelleted on glass slides by centrifugation at 500 rpm (400*g*) for 5 minutes using a cytospin system (Thermo Shandon). Cells were fixed in cold absolute acetone and methanol for 10 minutes. After fixation, cells were washed in PBS and then blocked for 60 minutes with 5% fetal bovine serum in PBS. Slides were then incubated with anti-LC3 antibody (Cell Signaling) at 4°C for 24 hours, washed in PBS, incubated with goat anti–mouse IgG-fluorescein isothiocyanate for 1 hour at 4°C, and analyzed using Nikon E800 fluorescence microscopy. Images were taken with objective lenses: N Plan 60×/1.25 oil, using a SPOT Insight QE model camera with SPOT Advanced acquisition software (Diagnostic Instruments), as previously described.[16,17]

### Detection and quantification of AVOs with acridine orange staining

Autophagy is characterized by sequestration of cytoplasmic proteins and development of acidic vesicular organelles (AVOs). To detect and quantify AVOs in CAL-101– or 3-MA–treated cells, we performed vital staining for 15 minutes with acridine orange at a final concentration of 1 μg/mL. Samples were examined under a fluorescence microscope.[18-20]

### Angiogenesis assay

The antiangiogenic activity of CAL-101 was determined using an in vitro Angiogenesis Assay Kit (Chemicon International). Human umbilical vein endothelial cells (HUVECs) and endothelial growth media were obtained from Lonza Walkersville. HUVECs were cultured with CAL-101 on polymerized matrix gel at 37°C. After 8 hours, tube formation was evaluated using Leica DM IL microscopy (Leica Microsystems) and analyzed with IM50 software (Leica Microsystems Imaging Solutions). HUVEC cell migration and rearrangement were visualized, and the number of branching points counted.

### Western blotting

MM cells were cultured with or without CAL-101, harvested, washed, and lysed using radioimmunoprecipitation assay buffer, 2mM $Na_3VO_4$, 5mM NaF, and 1mM phenylmethylsulfonyl fluoride (5 mg/mL), as described previously.[21] Whole-cell lysates were subjected to sodium dodecyl sulfate–polyacrylamide gel electrophoresis (SDS-PAGE) separation, transferred to Pure Nitrocellulose membranes (Bio-Rad Laboratories), and immunoblotted with anti-AKT, phospho(p)-AKT (Ser473, Thr 308), ERK1/2, P-ERK1/2, P-PDK1, STAT, P-STAT, P-FKRHL, P-70S6K, LC3, PARP, caspase 3, 8, and 9, as well as PI3K/p110α antibodies (Cell Signaling); anti-p110β, PI3K/p110δ, glyceraldehyde 3-phosphate dehydrogenase (GAPDH), α-tubulin, and actin Abs (Santa Cruz Biotechnology); anti-p110γ Ab (Alexis); and anti-LC3 Ab (Abgent).

### ELISA

Cytokine secretion by human BMSCs cocultured with MM cells was assessed by enzyme-linked immunosorbent assay (ELISA). BMSCs were cultured in 96-well plates with various concentrations of CAL-101, with or without INA-6 cells. After 48 hours, supernatants were harvested and stored

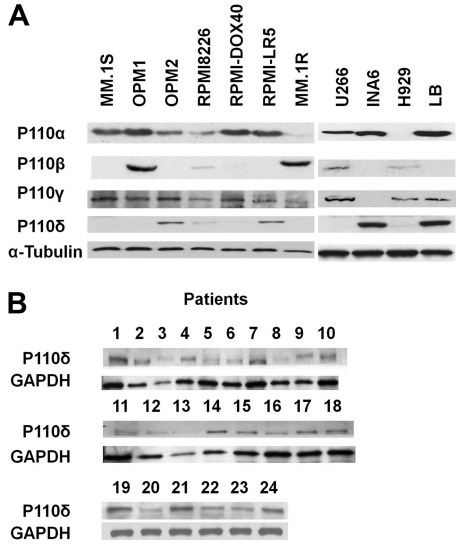


**Figure 1. Expression of p110δ in MM cell lines and in patient MM cells.** (A) Expression of p110α, β, γ, and δ in multiple myeloma (MM) cell lines was detected by immunoblotting using specific Abs. Anti–α-tubulin monoclonal antibody served as a loading control. (B) p110δ in patient MM cells was detected by immunoblotting using anti-p110δ Ab. Anti-GAPDH monoclonal antibody served as a loading control.

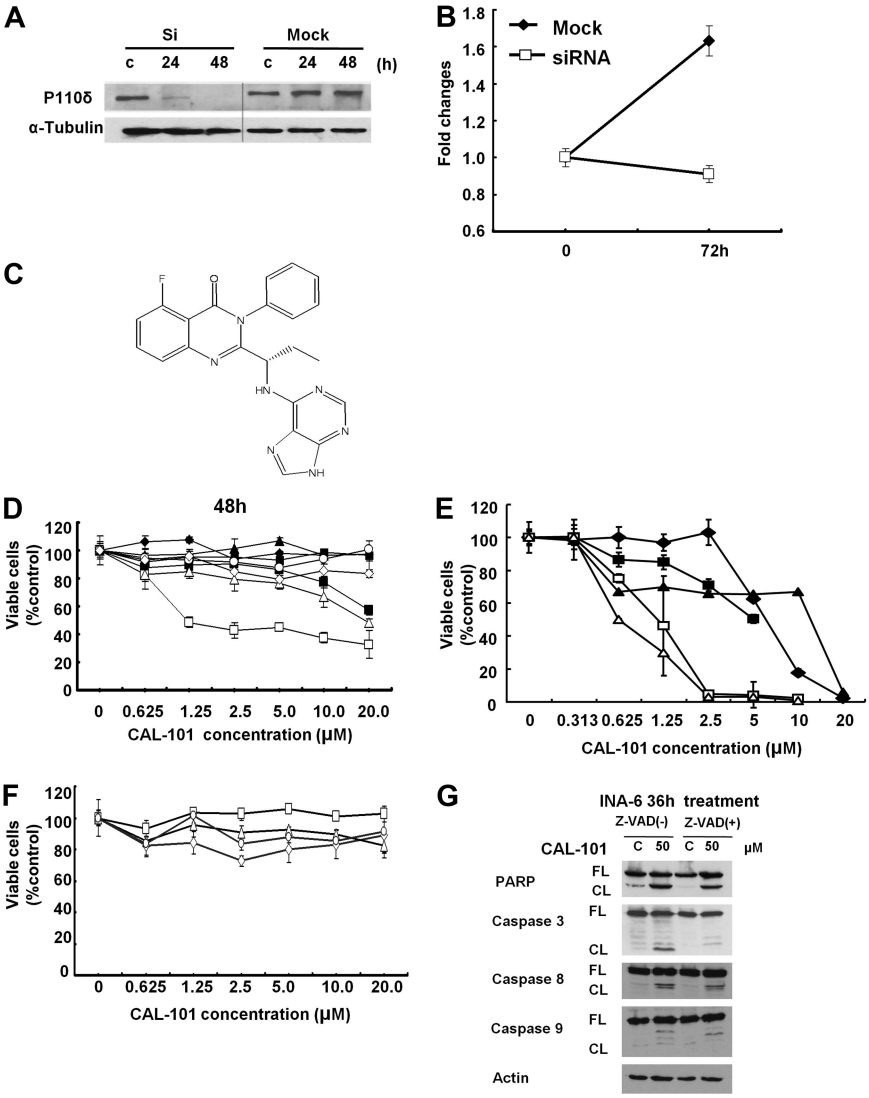


**Figure 2. Selective cytotoxicity of CAL-101 against p110δ-positive MM cell lines and patient MM cells.** (A) INA-6 cells were transfected with p110δ siRNA (Si) or control siRNA (Mock). After 24 hours, expression of p110δ was determined by Western blot analysis. Vertical lines have been inserted to indicate a repositioned gel line. (B) INA-6 cells were transfected with p110δ siRNA or control siRNA and then cultured for 72 hours. Cell growth was assessed by MTT assay. Data are mean ± SD of triplicate cultures, expressed as fold of control. (C) The chemical structure and PI3K assay profiling data of CAL-101. (D) LB (□), INA-6 (△), RPMI 8226(○), OPM2 (◇), H929 (●), U266 (◆), RPMI-LR5 (▲), and OPM1 (■) MM cells were cultured with or without CAL-101 (0-20μM) for 48 hours. (E) Patient MM cells isolated from BM by negative selection were cultured with CAL-101 for 48 hours. (F) PBMCs isolated from healthy donors were cultured with CAL-101 (0-20μM) for 72 hours. Data are mean ± SD viability, assessed by MTT assay of triplicate cultures, expressed as percentage of untreated controls. (G) INA-6 cells were cultured with or without CAL-101 (50μM for 36 hours ± Z-VAD-fmk). Total cell lysates were subjected to immunoblotting using anti–caspases 3, 8, and 9, PARP, and actin Abs. FL indicates full-length protein; and CL, cleaved protein.

at −80°C. Cytokines were measured using Duo set ELISA Development Kits (R&D Systems). All measurements were carried out in triplicate.

### Human cytokine array

The cytokine levels in culture supernatants were assessed using Proteome Profiler Antibody Arrays Panel A (R&D Systems). Supernatants from cocultures with BMSCs were incubated for 4 hours with membranes arrayed with Abs against 37 cytokines, according to the manufacturer's instructions.

### Murine xenograft models of human MM

CB17 SCID mice (48-54 days old) were purchased from Charles River Laboratories. All animal studies were conducted according to protocols approved by the Animal Ethics Committee of the Dana-Farber Cancer Institute. Mice were inoculated subcutaneously in the right flank with $3 \times 10^6$ LB cells in 100 μL RPMI 1640. When tumors were palpable, mice were assigned into the treatment groups receiving 10 mg/kg or 30 mg/kg gavages twice daily; and 7 mice in the control group receiving vehicle alone. Caliper measurements of the longest perpendicular tumor diameters were performed every alternate day to estimate the tumor volume using the following formula representing the 3-dimensional volume of an ellipse: $4/3 \times (\text{width}/2)^2 \times (\text{length}/2)$. Animals were killed when tumors reached 2 cm or the mice appeared moribund. Survival was evaluated from the first day of treatment until death. Tumor growth was evaluated using caliper measurements from the first day of treatment until day of first death, which was day 12 for the control group and days 17 and 19 for the treatment groups. The images were captured with a Canon IXY digital 700 camera. Ex vivo analysis of tumor images was captured with a Leica DM IL microscope and Leica DFC300 FX camera at 40×/0.60 (Leica).

Human fetal bone grafts were implanted into CB17 SCID-mice (SCID-hu), as previously described.[22] Four weeks after bone implantation, $2.5 \times 10^6$ INA-6 cells were injected directly into the human BM cavity in the graft in a final volume of 100 μL of RPMI 1640 medium. An increase in the levels of soluble human IL-6 receptor (shuIL-6R) from INA-6 cells was used as an indicator of MM cell growth and burden of disease in SCID-hu mice. Mice developed measurable serum shuIL-6R approximately 4 weeks after INA-6 cell injection and then received either 10 or 30 mg/kg drug or vehicle alone daily for 7 weeks. Blood samples were collected and assessed for shuIL-6R levels using an ELISA (R&D Systems).

### Statistical analysis

Statistical significance was determined by Dunn multiple comparison tests. The minimal level of significance was $P$ less than .05. Survival was assessed using Kaplan-Meier curves and log-rank analysis. The combined effect of CAL-101 and bortezomib was analyzed by isobologram analysis using the CalcuSyn software program (Biosoft; Version 2.0); a combination index less than 0.7 indicates a synergistic effect, as previously described.[23,24]

**Table 1. Kinase inhibition profile of CAL-101**

| | Fold-selectivity, PI3K | | | | | | | | |
|---|---|---|---|---|---|---|---|---|---|
| $IC_{50}$ (nM) | Class I | | | Class II | Class III | Class IV | | Others | |
| p110δ | p110α | p110β | p110γ | CIIβ | hVPS34 | DNA-PK | mTOR | PIP5Ka | PIP5Kb |
| 2.5 | > 300× | > 200× | > 40× | > 400× | > 400× | > 3000 × | > 4000 × | > 400 × | > 400 × |

CAL-101 shows PI3K/p110δ selectivity in kinase profiling assay.

## Results

### p110δ is highly expressed in patient MM cells

To assess PI3K/p110 expression, we used Abs against recombinant human PI3K/p110α, β, γ, and δ proteins with specific immunoreactivity against these isoforms (supplemental Figure 2). We specifically evaluated the expression of p110δ in 11 MM cell lines (MM.1S, OPM1, OPM2, RPMI8226, DOX40, LR5, MM.1R, U266, INA-6, H929, and LB), as well as 24 patient MM samples. INA-6 and LB cells strongly expressed p110δ, whereas MM.1S, OPM1, MM.1R, Dox40, U266, or H929 lacked p110δ expression (Figure 1A). p110δ expression in MM.1S and LB cells was confirmed by immunofluorescence analysis (supplemental Figure 3). Western blotting revealed no correlation between p110δ expression and expression of the other isoforms (α, β, and γ). Importantly, all patient MM cells also expressed p110δ (Figure 1B).

### CAL-101 has selective cytotoxicity against cells with p110δ

We next examined the growth-inhibitory effect of p110δ knockdown in INA-6 cells. Transfection with p110δ siRNA, but not mock siRNA, down-regulated p110δ and inhibited MM cell growth at 72 hours (Figure 2A-B). We similarly examined the growth inhibitory effect of p110δ specific small molecule inhibitor CAL-101 (Figure 2C; Table 1; and supplemental Figure 4) in MM cell lines, PBMCs, and patient MM cells. CAL-101 induced cytotoxicity against LB and INA-6 MM cells (p110δ-positive) in a dose- and time-dependent fashion; in contrast, minimal cytotoxicity was noted in p110δ-negative cell lines (Figure 2D). Importantly, CAL-101 also induced cytotoxicity against 5 patient MM cells (Figure 2E), without cytotoxicity in PBMCs from 4 healthy volunteers at concentrations up to 20μM (Figure 2F). These results strongly suggest that sensitivity to CAL-101 is associated with p110δ expression and suggest a favorable therapeutic window. To determine whether the cytotoxicity induced by CAL-101 is via apoptosis, we examined cleavage of caspases and PARP by Western blot analysis. Treatment of INA-6 cells with CAL-101 (50μM for 36 hours) induced cleavage of caspases 8, 9, and 3 and PARP. Conversely, the pan-caspase inhibitor z-VAD-fmk (50μM) blocked CAL-101-induced caspase and PARP cleavage (Figure 2G). Significantly increased cleavage of caspases and PARP was observed in INA-6 MM cells with prolonged CAL-101 treatment (120 hours; supplemental Figure 5). These results indicate that cytotoxicity triggered by CAL-101 is mediated, at least in part, via caspase-dependent (both intrinsic and extrinsic) apoptosis.

### Inhibition of AKT and ERK phosphorylation by CAL-101

Because we have previously shown that pan PI3K inhibitor LY294002 inhibits both AKT and ERK,[14,25,26] we next examined whether CAL-101 inhibits these pathways in INA-6 cells. As expected, CAL-101 significantly blocked phosphorylation of AKT and ERK1/2 in p110δ-positive INA-6 cells (Figure 3A) but did not affect phosphorylation of AKT or ERK in MM.1S cells with low expression of p110δ (Figure 3B). CAL-101 also significantly

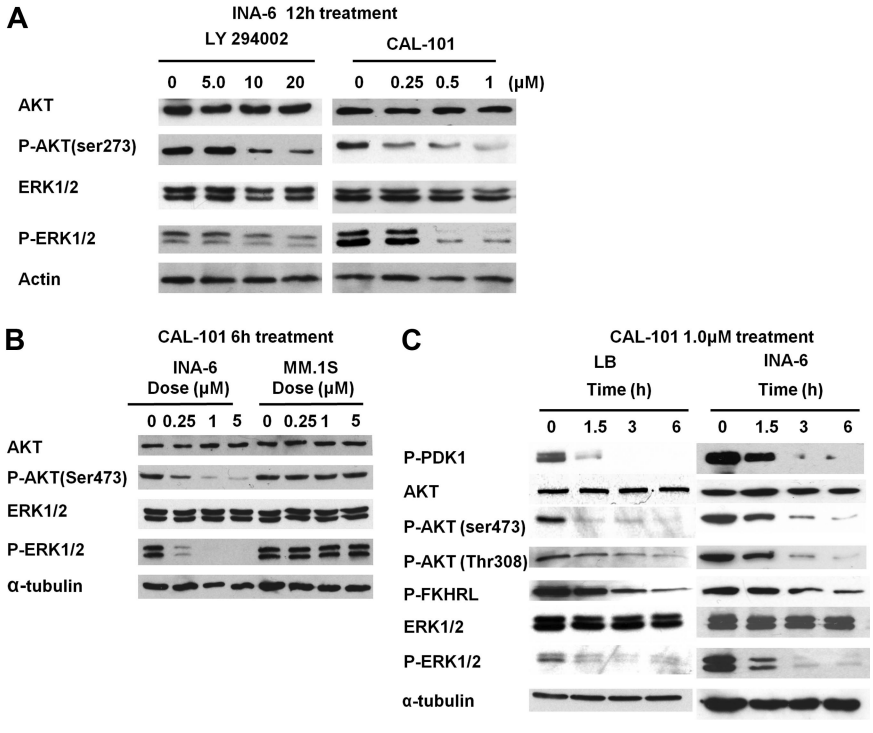


**Figure 3. CAL-101 inhibits the PI3K/Akt and ERK pathway.** (A) INA-6 cells were cultured with CAL-101 (0-1.0μM) or LY294002 (0-20μM) for 12 hours. Actin Ab was used as a loading control. (B) INA-6 and MM.1S cells were cultured with CAL-101 (0-5.0μM) for 6 hours. (C) LB and INA-6 cells were cultured with CAL-101 (1.0μM) for 0 to 6 hours. Whole-cell lysates were subjected to immunoblotting using AKT, P-AKT (Ser473 and Thr308), ERK1/2, P-ERK1/2, P-PDK1, and P-FKHRL Abs. α-Tubulin is used as a loading control.

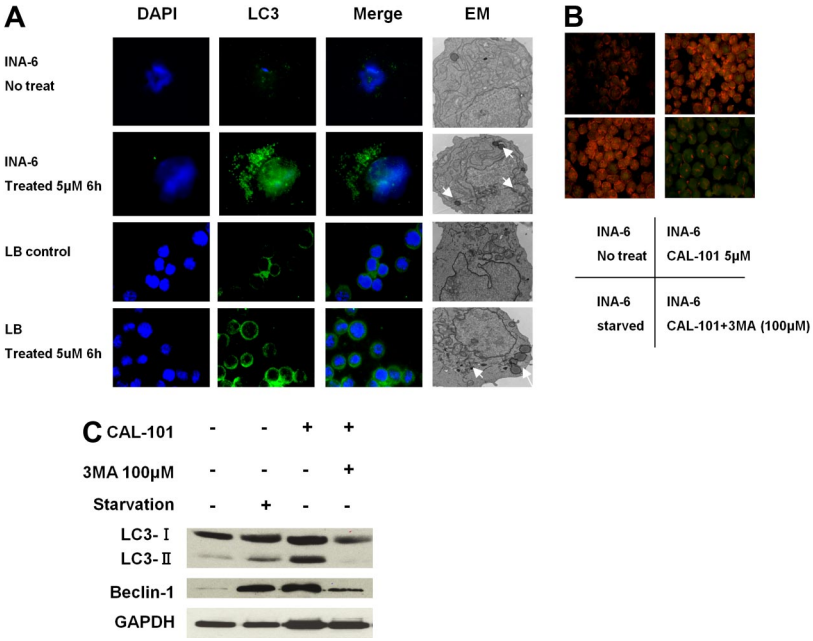


**Figure 4. CAL-101 induces autophagy.** (A) INA-6 and LB MM cells were treated with 5μM CAL-101 for 6 hours. CAL-101 treatment induced LC3 accumulation in LB and INA-6 cells, evidenced by fluorescence microscopy or transmission electron microscopy. Autophagosome formation was defined by the accumulation of LC3; arrows indicate autophagosomes. (B) INA-6 cells were treated with 5μM CAL-101 or serum starvation for 6 hours with or without 100μM 3-MA, stained with 1 μg/mL acridine orange for 15 minutes, and analyzed by fluorescence microscopy. (C) LC3 and beclin-1 protein levels were determined by Western blotting using LC3 and beclin1 Abs of lysates from INA-6 cells treated with CAL-101, with or without 3-MA. GAPDH served as a loading control.

inhibited phosphorylation of upstream PDK-1 and downstream FKHRL in INA-6 and LB MM cells in a time- and dose-dependent fashion (Figure 3C), further confirming inhibition of a both PI3K/AKT and ERK pathways in these cells.

### CAL-101 triggers both apoptosis and autophagy

Because AKT also regulates autophagy,[27,28] we further investigated whether CAL-101 induced autophagy in LB and INA-6 MM cells. Immunofluorescence analysis showed markedly increased LC3 staining in INA-6 and LB cells triggered by CAL-101 (5μM for 6 hours) treatment (Figure 4A). Electron microscopic analysis also showed increased autophagic vacuoles (arrows) in MM cells treated with CAL-101. Because autophagy is characterized as AVO development, we next carried out acridine orange staining. As shown in Figure 4B, vital staining with acridine orange revealed development of AVOs in CAL-101-treated LB and INA-6 cells. Moreover, markedly increased LC3-II and Beclin1 protein were detected in INA-6 MM cells after 6 hours of treatment with CAL-101, which was blocked by 3-MA autophagic inhibitor (Figure 4C). No cytotoxicity in INA-6 and LB cells was induced by 3-MA at concentrations up to 100μM (supplemental Figure 6). These results indicate that CAL-101 induces development of AVOs and autophagy at earlier time points than induction of caspase/PARP cleavage.

### CAL-101 inhibits paracrine MM cell growth with BMSCs

Because IL-6 and IGF-1 induce growth and antiapoptosis in MM cells, we next examined whether CAL 101 overcomes the effects of these cytokines in INA-6 and LB MM cells.[14,23] Neither IL-6 nor IGF-1 protected against the growth inhibition induced by CAL-101 (supplemental Figure 7A-B). Because we have also shown that the BM microenvironment confers proliferation and drug resistance in MM,[29,30] we also examined the MM cell growth-inhibitory effect of CAL-101 in the presence of BMSCs. Importantly, CAL-101 inhibited growth and cytokine secretion (Figure 5A-B; supplemental Figure 8), as well as phosphorylation of AKT and ERK (supplemental Figure 7C), induced by BMSCs. In contrast, no significant growth inhibition in BMSCs was noted (supplemental Figure 9). These results indicate that CAL-101 blocks paracrine MM cell growth in the context of the BM microenvironment.

### CAL101 inhibits HUVEC tubule formation

We next investigated the effect of p110δ inhibition on angiogenesis. HUVECs were treated with 0, 1.0, or 10μM of CAL-101 for 8 hours, and tube formation by endothelial cells was evaluated (Figure 5C). CAL-101 inhibited capillary-like tube formation in a

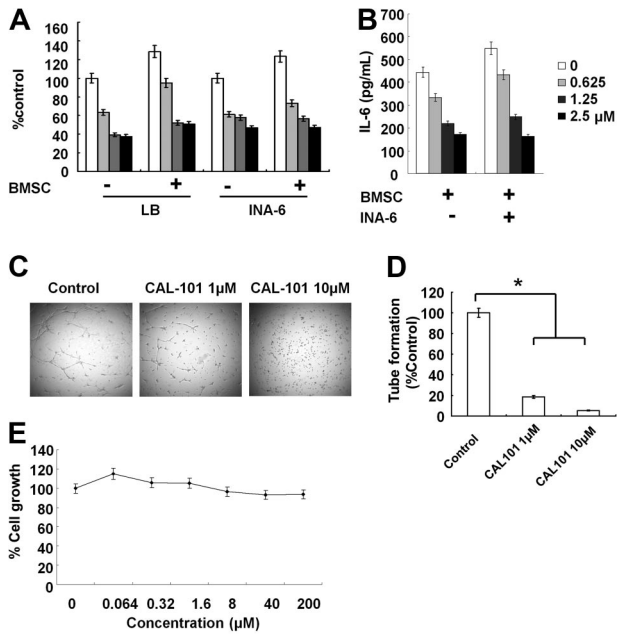


**Figure 5. CAL-101 inhibits paracrine MM cell growth and angiogenesis.** (A) LB and INA-6 MM cells were cultured for 48 hours with control media and with 2.5, 5, and 10μM CAL-101 in the presence or absence of BMSCs. DNA synthesis was determined by [3H]-thymidine incorporation. Data are mean ± SD of triplicate cultures. (B) IL-6 in culture supernatants from BMSCs treated with CAL101 (0-2.5μM) was measured by ELISA. Error bars represent SD. (C) HUVECs were cultured with or without 1.0 or 10μM CAL-101 for 8 hours, and tube formation was assessed by microscopy. (D) HUVECs were plated on Matrigel-coated surfaces and allowed to form tubules for 8 hours in the presence or absence of CAL-101 (1.0 and 10μM). Endothelial cell tube formation was measured by microscopic analysis. *$P < .005$. (E) HUVECs were cultured with CAL-101 (0-200μM) for 48 hours, and viability was assessed by MTT assay. Data are mean ± SE of triplicate wells from a representative experiment.

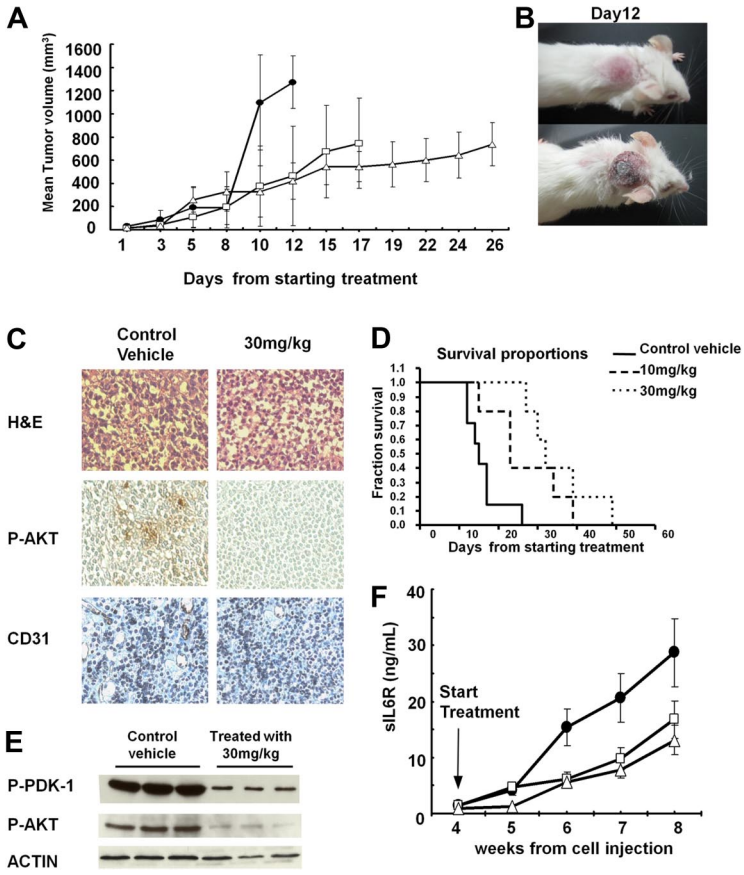


**Figure 6. In vivo efficacy of IC488743 treatment of human MM xenografts in SCID mice.** (A) Mice injected with $5 \times 10^6$ LB cells were treated orally twice a day with control vehicle (●), and IC488743 10 mg/kg (□) or 30 mg/kg (○). Mean tumor volume was calculated as in "Murine xenograft models of human MM." Error bars represent SD. (B) Representative whole-body images from a mouse treated for 12 days with control vehicle (top panel) or IC488743 (30 mg/kg; bottom panel). (C) Tumors harvested from IC488743 (30 mg/kg) treated mouse (right panel) and control mouse (left panel) were subjected to immunohistochemical analysis using CD31 and P-AKT Abs. CD31 and P-AKT positive cells are dark brown. (D) Mice were treated with IC488743 10 mg/kg (hyphenated line), 30 mg/kg (dotted line), or control vehicle (solid line). Survival was evaluated from the first day of treatment until death using Kaplan-Meier curves. (E) Tumor tissues were harvested from mice treated with control vehicle or IC488743 (30 mg/kg). Protein levels of phosphorylated of PDK-1 and AKT (Ser473) were determined by Western blotting of cell lysates. Actin was used as a loading control. (F) Growth of INA-6 cells engrafted in human bone chips in SCID mice was monitored by serial serum measurements of shuIL-6R. Mice were treated with IC488743 10 mg/kg (□), 30 mg/kg (△), or control vehicle (●), and shuIL-6R levels were determined weekly by ELISA. Error bars represent SD.

dose-dependent fashion ($P < .05$; Figure 5D), without associated cytotoxicity (Figure 5E). Phosphorylation and expression of AKT and ERK1/2 were markedly down-regulated in HUVECs by CAL101 treatment (supplemental Figure 10). These findings suggest that CAL-101 can inhibit angiogenesis, associated with down-regulation of AKT and ERK activity.

### IC488743 inhibits human MM cell growth in vivo

The in vivo efficacy of p110δ inhibitor was next evaluated in our xenograft model in which SCID mice are injected subcutaneously with human MM cells. IC488743 (p110δ inhibitor) significantly reduced MM tumor growth in the treatment group (n = 7) compared with control mice (n = 7). Comparison of tumor volumes showed statistically significant differences between control versus treatment groups (vs 10 mg/kg, $P < .05$; vs 30 mg/kg, $P < .01$; Figure 6A). Marked decrease in tumor growth in treated versus in control mice was observed at day 12 (Figure 6B). Kaplan-Meier curves and log-rank analysis showed a mean overall survival of 15 days (95% confidence interval, 12-17 days) in control mice versus 23 days (95% confidence interval, 15-34 days) and 32 days (95% confidence interval, 27-49 days) in the 10 mg/kg and 30 mg/kg IC488743-treated groups, respectively. A trend toward prolongation in mean OS was observed in treatment versus control groups (vs 10 mg/kg, $P = .086$; vs 30 mg/kg, $P = .056$; Figure 6D). Importantly, treatment with either the vehicle alone or IC488743 did not affect body weight (data not shown). In addition, we also confirmed by immunohistochemical (Figure 6C) and immunoblot (Figure 6E) analysis that IC488743 treatment (30 mg/kg) significantly inhibited p-Akt and p-PDK-1 in excised tumors, as well as significantly decreased CD31-positive cells and microvessel density ($P < .01$; Figure 6C).

To examine the activity of IC488743 on MM cell growth in the context of the human BM microenvironment in vivo, we next used a SCID-hu model in which IL-6-dependent INA-6 cells are directly injected into a human bone chip implanted subcutaneously in SCID mice. These SCID-hu mice were treated with IC488743 or vehicle alone daily for 4 weeks, and serum shuIL-6R monitored as a marker of tumor burden. As shown in Figure 6F, IC488743 treatment significantly inhibited tumor growth compared with vehicle control. Taken together, these data demonstrate that inhibition of p110δ by IC488743 significantly inhibits MM growth in vivo and prolongs survival.

### Combined CAL-101 with bortezomib mediates synergistic MM cytotoxicity

We next investigated whether combining CAL-101 with bortezomib induced synergistic MM cytotoxicity. Increasing concentrations of CAL-101 (1.5-5.0 μM) added to bortezomib (2.5, 5.0nM) triggered synergistic cytotoxicity in LB and INA-6 MM cells (Figure 7A; Table 2). Importantly, induction of phospho-Akt by bortezomib treatment was inhibited in the presence of CAL-101 (Figure 7B).

## Discussion

In this report, we demonstrate that patient MM cells express p110δ and, importantly, that p110δ specific inhibitors CAL-101 and IC488743 trigger MM cytotoxicity in vitro and in vivo, respectively. p110δ inhibition by CAL-101 potently induced cytotoxicity in p110δ-positive MM cells as well as in primary patient MM cells without cytotoxicity in PBMCs from healthy donors, suggesting a

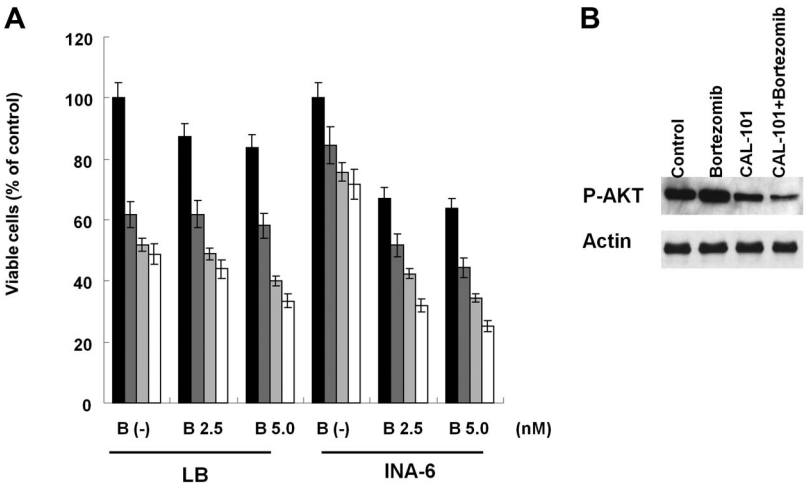


**Figure 7. CAL-101 enhances cytotoxicity of bortezomib.** (A) LB and INA-6 MM cells were cultured with medium (■) and with CAL101 1.25μM (■), 2.5μM (■), or 5μM (□) in the presence or absence of bortezomib (0-5nM). Cytotoxicity was assessed by MTT assay; data are mean ± SD of quadruplicate cultures. (B) INA-6 cells were treated with CAL-101 (5μM) and/or bortezomib (5nM) for 6 hours. Phosphorylation of AKT was determined by Western blotting of cell lysates using phospho-AKT (ser473) Ab. Actin served as a loading control.

favorable therapeutic index. An important downstream effector of PI3K is the serine/threonine protein kinase AKT, which is activated by phosphorylation of Thr308 in the activation loop of the kinase domain and Ser473 in the C-terminal tail.[31,32] Phosphorylation of both sites requires an interaction between the N-terminal pleckstrin homology domain of AKT and membrane phosphoinositide generated by PI3K.[8,33,34] CAL-101 inhibits both domains, suggesting that p110δ is the predominant isoform responsible for PI3K signaling in MM cell lines.

We and others have previously reported that IL-6 triggers proliferation of MM cells and protects against dexamethasone-induced apoptosis via activation of PI3K/AKT and MEK/ERK signaling cascades.[35-37] Here we showed that p110δ inhibition using CAL-101 blocked not only PI3K/AKT, but also MEK/ERK, pathways in MM cells. IGF-I also promotes MM cell proliferation and survival; however, neither IL-6 nor IGF-I protects against CAL-101-induced cytotoxicity, suggesting that CAL-101 can overcome the protective effects of these cytokines in the BM milieu. We further evaluated the impact of the BM microenvironment on the antitumor activity of CAL-101 using MM cells cocultured with BMSCs. CAL-101 both induced MM cytotoxicity in the presence of BMSCs and significantly inhibited the secretion of IL-6 from BMSCs, suggesting that inhibition of p110δ can both inhibit growth and overcome drug resistance in the BM milieu.

We next evaluated the in vivo efficacy of p110δ inhibitor in SCID-hu mice implanted with fetal bone chips engrafted with INA-6 MM cells.

**Table 2. CAL-101 with bortezomib triggers synergistic cytotoxicity**

| | Bortezomib (nM) | CAL-101 (μM) | Fa | CI |
|---|---|---|---|---|
| **LB** | | | | |
| | 2.5 | 1.25 | 0.39 | 0.57 |
| | 2.5 | 2.5 | 0.52 | 0.58 |
| | 2.5 | 5 | 0.57 | 0.67 |
| | 5 | 1.25 | 0.42 | 0.88 |
| | 5 | 2.5 | 0.60 | 0.25 |
| | 5 | 5 | 0.67 | 0.22 |
| **INA-6** | | | | |
| | 2.5 | 1.25 | 0.49 | 0.31 |
| | 2.5 | 2.5 | 0.58 | 0.48 |
| | 2.5 | 5 | 0.69 | 0.54 |
| | 5 | 1.25 | 0.56 | 0.73 |
| | 5 | 2.5 | 0.66 | 0.42 |
| | 5 | 5 | 0.75 | 0.31 |

LB and INA-6 cells were treated with bortezomib (2.5-5nM) and/or CAL-101 (1.25-5.0μM). Cytotoxicity was assessed by MTT assay. CI indicates combination index; and Fa, affected fraction. All doses show CI $< 1$.

This model recapitulates the human BM microenvironment with human IL-6/BMSC-dependent growth of INA-6 human MM cells. We observed significant tumor growth inhibition in this model, evidenced by decreased serum shuIL-6R levels released by INA-6 cells, confirming that p110δ inhibition blocks the MM growth-promoting activity of the BM microenvironment in vivo.

We also evaluated the role of PI3K, specifically p110 isoform, in angiogenesis.[38,39] Endothelial cells are an essential regulator of angiogenesis for tumor growth. Both Akt and ERK pathways are associated with endothelial cell growth and regulation of angiogenesis[40]; and importantly, endothelial cells express p110δ.[41] We here demonstrated that CAL-101 blocks in vitro capillary-like tube formation, associated with down-regulation of Akt phosphorylation. Furthermore, we confirmed the inhibitory effect on angiogenesis by immunohistochemical analysis for CD31 expression in our human MM xenograft model. These results suggest that IC488743 can inhibit angiogenesis in vivo via suppression of Akt pathway.

Autophagy degrades cellular components, recycles cellular constituents, and responds to various cellular stress.[42] We here shown that LC3-II, a hallmark of autophagy, is induced by CAL-101 treatment in p110δ-positive MM cell lines. Importantly, CAL-101 treatment resulted in a marked increase in autophagy, evidenced by the presence of autophagic vacuoles in the cytoplasm, formation of AVOs, membrane association of microtubule-associated LC3-I protein with autophagosomes, and a marked induction of LC3-II protein. Electron microscopic analysis confirmed that CAL-101 induced autophagosomes. LC3-II was expressed through LC3-I conversion. Conversely, autophagy induced by CAL-101 was suppressed by 3-MA, a specific inhibitor of autophagy. These studies suggest that early cytotoxic effects of CAL-101 are associated with autophagy.

Bortezomib was Food and Drug Administration approved for relapsed/refractory, relapsed, and newly diagnosed MM in 2003, 2005, and 2007,[43-45] respectively. However, some patients do not respond and others acquire resistance. We here demonstrated that CAL-101 can synergistically augment bortezomib-induced MM cytotoxicity. Specifically, CAL-101 inhibits bortezomib-induced phosphorylation of AKT, suggesting the promise of this combination to overcome clinical proteasome resistance.

In conclusion, we demonstrate, for the first time, that p110δ inhibitor CAL-101 induces cytotoxicity in MM cell lines and patient MM cells, as well as overcomes the protective effects of IL-6, IGF-1, and BMSCs. It induces autophagy and synergistic cytotoxicity with bortezomib. In addition, IC488743 inhibits both

tumor growth and prolongs survival in our murine xenograft and SCID-hu models of human MM. Taken together, these results provide the preclinical rationale for the clinical evaluation of p110δ inhibitor, alone and in combination with bortezomib, to improve patient outcome in MM.

## Acknowledgments

This work was supported by the National Institutes of Health Specialized Programs of Research Excellence (grants IP50 CA10070, PO-1 CA78378, and RO-1 CA50947), the Multiple Myeloma Research Foundation (T.H., K.C.A.), and the LeBow Family Fund to Cure Myeloma (K.C.A.).

## Authorship

Contribution: H.I., T.H., and K.C.A. performed experiments, designed the research, and wrote the paper; M.F., G.P., H.Y., Y.O., T.K., L.S., S.V., D.C., E.C., G.G., and N.S.R. designed the research and analyzed data; P.R. and N.C.M. designed the research; and B.J.L., K.D.P., and N.A.G. contributed vital new reagents.

Conflict-of-interest disclosure: The authors declare no competing financial interests.

Correspondence: Kenneth C. Anderson, Jerome Lipper Multiple Myeloma Center, Harvard Medical School, Dana-Farber Cancer Institute, 44 Binney St, Boston, MA 02115-6084; e-mail: kenneth_anderson@dfci.harvard.edu.

## References

1. Tai YT, Podar K, Catley L, et al. Insulin-like growth factor-1 induces adhesion and migration in human multiple myeloma cells via activation of beta1-integrin and phosphatidylinositol 3′-kinase/AKT signaling. *Cancer Res.* 2003;63(18):5850-5858.
2. Hideshima T, Richardson P, Anderson KC. Novel therapeutic approaches for multiple myeloma. *Immunol Rev.* 2003;194:164-176.
3. Podar K, Tai YT, Cole CE, et al. Essential role of caveolae in interleukin-6- and insulin-like growth factor I-triggered Akt-1-mediated survival of multiple myeloma cells. *J Biol Chem.* 2003;278(8):5794-5801.
4. Hsu JH, Shi Y, Frost P, et al. Interleukin-6 activates phosphoinositol-3′ kinase in multiple myeloma tumor cells by signaling through RAS-dependent and, separately, through p85-dependent pathways. *Oncogene.* 2004;23(19):3368-3375.
5. Petiot A, Ogier-Denis E, Blommaart EF, Meijer AJ, Codogno P. Distinct classes of phosphatidylinositol 3′-kinases are involved in signaling pathways that control macroautophagy in HT-29 cells. *J Biol Chem.* 2000;275(2):992-998.
6. Byfield MP, Murray JT, Backer JM. hVps34 is a nutrient-regulated lipid kinase required for activation of p70 S6 kinase. *J Biol Chem.* 2005;280(38):33076-33082.
7. Vanhaesebroeck B, Alessi DR. The PI3K-PDK1 connection: more than just a road to PKB. *Biochem J.* 2000;346(3):561-576.
8. Klippel A, Kavanaugh WM, Pot D, Williams LT. A specific product of phosphatidylinositol 3-kinase directly activates the protein kinase Akt through its pleckstrin homology domain. *Mol Cell Biol.* 1997;17(1):338-344.
9. Chen JS, Zhou LJ, Entin-Meer M, et al. Characterization of structurally distinct, isoform-selective phosphoinositide 3′-kinase inhibitors in combination with radiation in the treatment of glioblastoma. *Mol Cancer Ther.* 2008;7(4):841-850.
10. Hafner C, Lopez-Knowles E, Luis NM, et al. Oncogenic PIK3CA mutations occur in epidermal nevi and seborrheic keratoses with a characteristic mutation pattern. *Proc Natl Acad Sci U S A.* 2007;104(33):13450-13454.
11. Lannutti BJ. CAL-101, a potent selective inhibitor of the p110d isoform of phosphatidylinositol 3-kinase, attenuates PI3K signaling and inhibits proliferation and survival of Acute Lympoblastic Leukemia in addition to a range of other hematological malignancies. *Am Soc Hematol.* 2008; 112. Abstract 16.
12. Flinn IW, Furman RR, Brown JR, Lin TS, Bello C, Giese NA. Preliminary evidence of clinical activity in a phase I study of CAL-101, a selective inhibitor of the p110delta isoform of phosphatidylinositol 3-kinase (P13K), in patients with select hematologic malignancies. *J Clin Oncol.* 2009; 27(A3543).
13. Hideshima T, Chauhan D, Hayashi T, et al. Antitumor activity of lysophosphatidic acid acyltransferase-beta inhibitors, a novel class of agents, in multiple myeloma. *Cancer Res.* 2003;63(23):8428-8436.
14. Hideshima T, Chauhan D, Podar K, Schlossman RL, Richardson P, Anderson KC. Novel therapies targeting the myeloma cell and its bone marrow microenvironment. *Semin Oncol.* 2001;28(6):607-612.
15. Podar K, Gouill SL, Zhang J, et al. A pivotal role for Mcl-1 in bortezomib-induced apoptosis. *Oncogene.* 2008;27(6):721-731.
16. Ikeda H, Sasaki Y, Kobayashi T, et al. The role of T-fimbrin in the response to DNA damage: silencing of T-fimbrin by small interfering RNA sensitizes human liver cancer cells to DNA-damaging agents. *Int J Oncol.* 2005;27(4):933-940.
17. Kiziltepe T, Hideshima T, Catley L, et al. 5-Azacytidine, a DNA methyltransferase inhibitor, induces ATR-mediated DNA double-strand break responses, apoptosis, and synergistic cytotoxicity with doxorubicin and bortezomib against multiple myeloma cells. *Mol Cancer Ther.* 2007;6(6):1718-1727.
18. Ollinger K, Roberg K. Nutrient deprivation of cultured rat hepatocytes increases the desferrioxamine-available iron pool and augments the sensitivity to hydrogen peroxide. *J Biol Chem.* 1997; 272(38):23707-23711.
19. Lambert LA, Qiao N, Hunt KK, et al. Autophagy: a novel mechanism of synergistic cytotoxicity between doxorubicin and roscovitine in a sarcoma model. *Cancer Res.* 2008;68(19):7966-7974.
20. Castino R, Davies J, Beaucourt S, Isidoro C, Murphy D. Autophagy is a prosurvival mechanism in cells expressing an autosomal dominant familial neurohypophyseal diabetes insipidus mutant vasopressin transgene. *FASEB J.* 2005;19(8):1021-1023.
21. Yasui H, Hideshima T, Raje N, et al. FTY720 induces apoptosis in multiple myeloma cells and overcomes drug resistance. *Cancer Res.* 2005; 65(16):7478-7484.
22. Urashima M, Chen BP, Chen S, et al. The development of a model for the homing of multiple myeloma cells to human bone marrow. *Blood.* 1997; 90(2):754-765.
23. Hideshima T, Catley L, Yasui H, et al. Perifosine, an oral bioactive novel alkylphospholipid, inhibits Akt and induces in vitro and in vivo cytotoxicity in human multiple myeloma cells. *Blood.* 2006; 107(10):4053-4062.
24. Hayashi T, Hideshima T, Akiyama M, et al. Arsenic trioxide inhibits growth of human multiple myeloma cells in the bone marrow microenvironment. *Mol Cancer Ther.* 2002;1(10):851-860.
25. Leleu X, Jia X, Runnels J, et al. The Akt pathway regulates survival and homing in Waldenstrom macroglobulinemia. *Blood.* 2007;110(13):4417-4426.
26. Giuliani N, Lunghi P, Morandi F, et al. Downmodulation of ERK protein kinase activity inhibits VEGF secretion by human myeloma cells and myeloma-induced angiogenesis. *Leukemia.* 2004;18(3):628-635.
27. Fazi B, Bursch W, Fimia GM, et al. Fenretinide induces autophagic cell death in caspase-defective breast cancer cells. *Autophagy.* 2008; 4(4):435-441.
28. Singletary K, Milner J. Diet, autophagy, and cancer: a review. *Cancer Epidemiol Biomarkers Prev.* 2008;17(7):1596-1610.
29. Okawa Y, Hideshima T, Steed P, et al. SNX-2112, a selective Hsp90 inhibitor, potently inhibits tumor cell growth, angiogenesis, and osteoclastogenesis in multiple myeloma and other hematologic tumors by abrogating signaling via Akt and ERK. *Blood.* 2009;113(4):846-855.
30. Hideshima T, Mitsiades C, Tonon G, Richardson PG, Anderson KC. Understanding multiple myeloma pathogenesis in the bone marrow to identify new therapeutic targets. *Nat Rev Cancer.* 2007;7(8):585-598.
31. Ballou LM, Lin HY, Fan G, Jiang YP, Lin RZ. Activated G alpha q inhibits p110 alpha phosphatidylinositol 3-kinase and Akt. *J Biol Chem.* 2003; 278(26):23472-23479.
32. Alessi DR, Kozlowski MT, Weng QP, Morrice N, Avruch J. 3-Phosphoinositide-dependent protein kinase 1 (PDK1) phosphorylates and activates the p70 S6 kinase in vivo and in vitro. *Curr Biol.* 1998;8(2):69-81.
33. Yano S, Tokumitsu H, Soderling TR. Calcium promotes cell survival through CaM-K kinase activation of the protein-kinase-B pathway. *Nature.* 1998;396(6711):584-587.
34. Vivanco I, Sawyers CL. The phosphatidylinositol 3-kinase AKT pathway in human cancer. *Nat Rev Cancer.* 2002;2(7):489-501.
35. Luo J, Manning BD, Cantley LC. Targeting the PI3K-Akt pathway in human cancer: rationale and promise. *Cancer Cell.* 2003;4(4):257-262.
36. Steelman LS, Pohnert SC, Shelton JG, Franklin RA, Bertrand FE, McCubrey JA. JAK/STAT, Raf/MEK/ERK, PI3K/Akt and BCR-ABL in cell cycle progression and leukemogenesis. *Leukemia.* 2004;18(2):189-218.
37. Cantley LC. The phosphoinositide 3-kinase pathway. *Science.* 2002;296(5573):1655-1657.
38. Rajkumar SV, Greipp PR. Prognostic factors in multiple myeloma. *Hematol Oncol Clin North Am.* 1999;13(6):1295-1314.

39. Ziche M. Role of nitric oxide in the angiogenesis of avascular tissue. *Osteoarthritis Cartilage.* 1999;7(4):403-405.

40. Shankar S, Srivastava RK. Involvement of Bcl-2 family members, phosphatidylinositol 3′-kinase/AKT and mitochondrial p53 in curcumin (diferulolylmethane)-induced apoptosis in prostate cancer. *Int J Oncol.* 2007;30(4):905-918.

41. Puri KD, Doggett TA, Douangpanya J, et al. Mechanisms and implications of phosphoinositide 3-kinase delta in promoting neutrophil trafficking into inflamed tissue. *Blood.* 2004;103(9):3448-3456.

42. Cui Q, Tashiro S, Onodera S, Minami M, Ikejima T. Oridonin induced autophagy in human cervical carcinoma HeLa cells through Ras, JNK, and P38 regulation. *J Pharmacol Sci.* 2007;105(4):317-325.

43. Richardson PG, Barlogie B, Berenson J, et al. A phase 2 study of bortezomib in relapsed, refractory myeloma. *N Engl J Med.* 2003;348(26):2609-2617.

44. Richardson PG, Mitsiades C, Hideshima T, Anderson KC. Proteasome inhibition in the treatment of cancer. *Cell Cycle.* 2005;4(2):290-296.

45. Mulligan G, Mitsiades C, Bryant B, et al. Gene expression profiling and correlation with outcome in clinical trials of the proteasome inhibitor bortezomib. *Blood.* 2007;109(8):3177-3188.